In vivo identification and validation of novel potential predictors for human cardiovascular diseases

Omar T. Hammouda[1,2], Meng Yue Wu[1], Verena Kaul[1], Thomas Thumberger[1] and Joachim Wittbrodt[1,*]

[1]Centre for Organismal Studies Heidelberg, Heidelberg University, Im Neuenheimer Feld 230, 69120 Heidelberg, Germany

[2]Heidelberg Biosciences International Graduate School, Heidelberg University, Im Neuenheimer Feld 501, 69120 Heidelberg, Germany

[*]Corresponding Author

Running title (40 char): Validating understudied GWAS heart genes

Final character count (with spaces): 19,306

17 Abstract

18 Genetics crucially contributes to cardiovascular diseases (CVDs), the global
19 leading cause of death. Since the majority of CVDs can be prevented by early
20 intervention there is a high demand for predictive markers. While genome wide
21 association studies (GWAS) correlate genes and CVDs after diagnosis and
22 provide a valuable resource for such markers, preferentially those with pre-
23 assigned function are addressed further. To tackle the unaddressed blind spot of
24 understudied genes, we particularly focused on the validation of heart GWAS
25 candidates with little or no apparent connection to cardiac function. Building on
26 the high conservation of basic heart function and underlying genetics from fish
27 to human we combined CRISPR/Cas9 genome editing of the orthologs of
28 human GWAS candidates in isogenic medaka with automated high-throughput
29 heart rate analysis. Our functional analyses of understudied human candidates
30 uncovered a prominent fraction of heart rate associated genes from adult human
31 patients displaying a heart rate effect in embryonic medaka already in the
32 injected generation. Following this pipeline, we identified 16 GWAS candidates
33 with potential diagnostic and predictive power for human CVDs.

34

35 Keywords: CRISPR / gene validation / GWAS / heart rate / high throughput
36 analysis

Introduction

Genetics crucially contributes to the development and progression of cardiovascular diseases (CVDs), the global leading cause of death (Kathiresan & Srivastava 2012; Cambien & Tiret 2007). Elevated resting heart rate in humans has been widely considered as a potential, modifiable risk factor of cardiovascular and all-cause mortality (Beere et al. 1984; DYER et al. 1980; MD et al. 2010; Gillum et al. 1991). Since the majority of CVDs can be prevented by early intervention (McGill et al. 2008) there is a high demand for diagnostic and predictive CVD markers. Genome wide association studies (GWAS) on human patients correlate genes and CVDs after diagnosis and provide a valuable resource for those putative markers (Eicher et al. 2015). However, genes with pre-assigned cardiac functions are usually more likely to be addressed further, while uncharacterized genes or those with no pre-existing evidence to the heart are often neglected. This is likely due to the lack of experimental pipelines for the rapid and robust validation of such markers with implications for heart function. Recently, we demonstrated the power of targeted genome editing in the small animal model system medaka (*Oryzias latipes*) to validate trabeculation-associated genes (Meyer et al. 2020). The ease of manipulation combined with robust acquisition and analysis pipelines highlight the power of using fish embryos in high-throughput applications (Gierten et al.

2020; Shankaran et al. 2018; Lessman 2011; Oxendine et al. 2006). Embryos of fish model systems undergo extrauterine development in a transparent egg. This allows to monitor heart development and heart rate non-invasively in live undisturbed embryos for an extended period of time. Heart development, function and physiology in fish, though simpler, is comparable to mammals (Nemtsas et al. 2010; Yonekura et al. 2018; Gut et al. 2017). Here we combined targeted genome editing via CRISPR/Cas9 (Stemmer et al. 2015) with automated high-throughput imaging and heart rate analysis in isogenic medaka embryos (Gierten et al. 2020) to enable functional analyses directly in the injected generation. We tested the performance our assay with a positive control (*nkx2-5*), evaluated the random discovery rate and analyzed 40 heart associated genes identified from human GWAS. Our assay uncovered that 57% of candidates assigned to human heart rate in GWAS also affected heart rate in fish embryos. We have thus experimentally validated understudied human GWAS candidates, identifying 16 genes with potential diagnostic and predictive power for human CVDs.

Results

For the straight forward functional validation of GWAS candidates we aimed at combining CRISPR/Cas9-mediated targeted gene inactivation in the injected

77 generation of medaka embryos with high content screening approaches to
78 validate the impact of the loss-of-function on the heart rate (Fig 1A). As a
79 positive control, we used the cardiac-specific homeobox-containing transcription
80 factor NKX2-5. In human patients, a single amino acid mutation in the
81 homeodomain (R141C) was previously associated with atrial septal defect
82 (ASD) and shown to cause delayed heart morphogenesis in adult mice
83 (Zakariyah et al. 2017). To test our high-throughput imaging and heart rate
84 analysis pipeline for functional *in vivo* gene validation in the injected generation,
85 we targeted the region orthologous to R141C in medaka embryos using the
86 CRISPR/Cas9 system (Stemmer et al. 2015). As a negative control, we targeted
87 the *oculocutaneous albinism* 2 locus (*oca2*) (Fukamachi et al. 2004) as a heart-
88 unrelated pigmentation gene. The apparent loss of eye pigmentation phenotype
89 (and degree of mosaicism) was used as a measure for the knock-out efficacy
90 (Lischik et al. 2019; Hammouda et al. 2019). Injections into medaka embryos
91 were performed at the 1-cell stage, resulting in CRISPR/Cas9-mediated
92 mutantions exhibiting a degree of genetic mosaicism in the injected embryos
93 hereafter referred to as crispants. To address the impact on the heart rate we
94 raised the medaka crispants until cardiac function was fully developed and the
95 heart rate had reached a plateau at 4 days post fertilization (Gierten et al. 2020)
96 (4 dpf; developmental stage ~31-32 (Iwamatsu 2004)) .

To assess changes in mean heart rate with statistical significance, we took advantage of a 96-well plate format, and imaged multiple biological replicates of crispant embryos (3 rows; n=36 per condition) as well as of *GFP mRNA* mock-injected siblings as internal plate control (2 rows; n=24) (Fig S1A). To assess heart function under different environmental conditions, embryos were imaged at two different temperatures (21 and 28°C, respectively). Heart rates of all embryos were quantitatively determined from the imaging data using the *HeartBeat* software and randomly selected embryos were genotyped to correlate CRISPR/Cas9 targeting (Hammouda et al. 2019).

While mock injected embryos did not show phenotypes, crispants of the positive control *nkx2-5* displayed a variety thereof. These ranged from global severe developmental delays to local cardiac malformations morphologically resembling the phenotypes previously observed in zebrafish *nkx2-5* mutants such as enlarged heart chambers (Fig 1B) (Targoff et al. 2013). Notably, in the negative control (*oca2* crispants) neither cardiac nor developmental phenotypes were observed (Fig 1B), indicating that genome targeting of *oca2* as well as injection and handling of the embryos did not impact on heart and general development per se. Quantitative comparison of cardiac function revealed an overall elevation in the mean heart rate of *nkx2-5* crispants (21°C 99.7 bpm, 28°C 166 bpm) compared to mock control siblings (21°C 96.1 bpm, 28°C 164

bpm) with a significant ($p = 0.0074$) difference at 21°C (Fig 1C; left panel). Notably, independent experimental replicates targeting the same *nkx2-5* exon with two different sgRNAs robustly yielded a significant heart rate phenotype at 21°C (Fig S1B-C). In contrast, the mean heart rate in *oca2* crispants was indifferent from mock control at either temperature (21°C 96.4 bpm, 28°C 165 bpm), validating *oca2* as bona fide negative control.

To avoid severe developmental delays in *nkx2-5* crispants to potentially skew heart rate comparisons, we further applied a developmental focusing filter. Only embryos having developed beyond stage 28 (Iwamatsu 2004), at which cardiac function was previously shown to have reached a functional plateau (Gierten et al. 2020), were chosen for statistical analysis. Developmental focusing, only excluded three embryos from the *nkx2-5* group which did not impact on the results (Fig 1C; right panel). These results underline the robustness of our pipeline and demonstrate its sensitivity to detect mild heart rate phenotypes reflecting cardiac function already at embryonic stages of medaka development.

Next, we determined the baseline probability of heart rate phenotypes by targeting a set of randomly selected genes with CRISPR/Cas9. From a total of 23622 annotated medaka coding genes in Ensembl (Yates et al. 2020), we used a random number generator to select 10 genes (Table 1). For each gene, a random

137 exon was chosen for targeting via CRISPR/Cas9. As before, we used 96-well
138 plates to test two target genes per plate. To control for potential heart rate
139 fluctuations in embryos within and across different experiments, we included
140 mock-injected siblings as internal plate control. Heart rates of target gene
141 crispants and control siblings were scored and the means were compared before
142 and after developmental focusing. Comparative heart rate analysis of the
143 randomly selected genes revealed a heart rate phenotype in two out of ten genes
144 at both temperatures measured (Fig 2, and Fig S2). Remarkably, both genes, the
145 *oxoglutarate dehydrogenase* (*ogdh*) and the *cell division control protein 42*
146 *homolog* (*cdc42)* have been previously associated with heart phenotypes in
147 human (GWAS) or were shown to play a role in heart function, respectively
148 (Thanassoulis et al. 2013; Qian et al. 2011; Li et al. 2017). These results confirm
149 the reliability of our assay to identify genes of a given set that affect cardiac
150 function. Of note, repeated rounds of random gene selection revealed a similar
151 mean baseline of 10-20% of selected genes being related to the heart in GWAS
152 or previous experimental reports.
153 We next applied our pipeline to interrogate a larger, targeted selection of genes
154 associated with cardiovascular diseases in human GWAS. We used GRASP
155 (Eicher et al. 2015), the genome-wide repository of associations between single
156 nucleotide polymorphisms (SNPs) and phenotypes, to compile a list of 40

157 candidate genes from human GWAS with a coding association to heart
158 phenotypes **(**hGWAS genes; Table 2). We focused on genes with no prior
159 experimental link to heart function, while including few known heart genes as
160 additional positive controls. To address the specificity of our approach, the
161 selected candidate genes were categorized according to their association into
162 general heart related (n=17) or related specifically to heart rate (n= 23; Table2).
163 Heart rates of candidate gene crispants and control injected siblings were scored
164 and compared before (Fig S4) and after developmental focusing (Fig 3A and
165 Figure S3). Across the hGWAS set of 40 genes, comparative heart rate analysis
166 showed statistically significant heart rate phenotypes in a total of 16 genes (Fig
167 3B). The five positive controls, known to play key roles in heart functions such
168 as cardiac contraction (*TTN* and *NACA*) and heart rate regulation (*CASQ2*,
169 *KCNH2* and *SCN5A*) (Itoh-Satoh et al. 2002; Park et al. 2010; Faggioni &
170 Knollmann 2012; Gianulis & Trudeau 2011; Zaklyazminskaya &
171 Dzemeshkevich 2016; Huttner et al. 2013) clearly responded in the assay.
172 Beyond known cardiac genes, we revealed new genes linked to various
173 biological functions (*CCDC141*, *GIGYF1*, *HOMEZ*, *MYRF*, *SMG6*, *CMYA5*,
174 *CNOT1*, *SLC17A3*, *TRAPPC12*, *SSPO* and *PADI4*) which up to now, had little
175 to no experimental evidence in cardiac function (Rathjens et al. 2020; Benson et
176 al. 2017; Yamaguchi et al. 2018; Elmen et al. 2020).

When analyzing the candidates according to their GWAS association ("heart rate" and "non-heart rate" phenotypes), we observed a strong positive correlation between the respective phenotypes observed in medaka crispants and the associated phenotype in adult human GWAS. The proportion of heart rate-associated genes in hGWAS that yield a heart rate phenotype in medaka (13/23) was elevated compared to the proportion of non-heart rate-associated genes yielding a heart rate phenotype (3/17). Even when considering the entire group, we observed a higher proportion of genes with an effect on heart rate in our targeted hGWAS gene set (16/40) compared to our randomly selected gene set (2/10) (Fig 3C). Taken together, phenotypes in early medaka embryos likely reflect risk factors in human adults, thus we uncovered functionally relevant heart rate phenotypes in previously uncharacterized genes.

Interestingly, analysis of *scn4ab* crispants displayed a bimodal heart rate distribution, with a population displaying roughly half the average heart rate at both recorded temperatures (Fig 4A). Visual inspection of the *scn4ab* embryos revealed an arrhythmic heart anomaly previously reported in zebrafish mutants (Huttner et al. 2013), i.e. an atrio-ventricular block (AV-block), characterized by a delay or disruption of impulse transmission from the atrium to the ventricle. Scoring the beat frequency of both heart chambers separately in individual

197 embryos exposed the impaired rhythm of atrial to ventricular contractions,
198 which resulted in a delay or even skipping of ventricular beats in the *scn4ab*
199 crispants but not in control siblings (Fig 4B). *scn4ab* crispants displayed various
200 severities of the AV-block from mild (regular heart beats with occasional beat
201 skipping), to moderate (consistent 2:1 atrial to ventricular contraction; Movie
202 S1), to severe (3:1 or more; Movie S2). Still heavily affected *scn4ab* crispants
203 survived until hatching. Impressively, the prevalence of the arrhythmia
204 phenotype in *scn4ab* crispants was markedly high, exceeding 90% of the
205 injected embryos, reflecting the high efficiency of the Cas9 and the high
206 penetrance of the mutations introduced. These results further underscore the
207 efficacy of using medaka crispant embryo analysis as a rapid validation tool to
208 identify genes with a functional link to human cardiac diseases.
209
210 Discussion
211 Most cardiovascular diseases can be prevented if diagnosed and treated early.
212 Previous studies have shown the importance of the resting heart rate as a vital
213 risk factor both in terms of prediction and prevention of CVDs (DYER et al.
214 1980; MD et al. 2010; Eppinga et al. 2016). An increase of 5 beats per minute
215 correlates with a 20% increase in risk of mortality (Eppinga et al. 2016), and

reducing the resting heart rate has proven to improve the clinical outcomes of various CVDs (Beere et al. 1984; MD et al. 2010).

Human GWAS have been performed in search of genetic determinants of CVDs, and although a wide array of candidate genes with various functions are being associated to heart phenotypes in human GWAS, further focus is usually turned to those few genes with pre-existing indication of cardiac function. Other associated genes with an unknown function or without a pre-existing functional link to the heart are often neglected and not pursued further, pushing all those into a blind spot, resulting in a negative loop of discovery. Thus, it is important to address the role of such genes in heart function through experimental validation in model organisms, in pursuit of novel markers for CVD diagnosis.

We address this blind spot of discovery by applying a high-throughput heart rate imaging and analysis pipeline coupled to a reverse genetic validation approach via CRISPR/Cas9 mediated mutagenesis in a genetically suited vertebrate model (Fig 1A).

F0 mutagenesis screens are becoming more and more popular (Teboul 2017; Shankaran et al. 2018; Wu et al. 2018; Heyde et al. 2020), largely due to the improvements in CRISPR/Cas9 gene targeting efficiency. Overall, gene targeting in medaka using CRISPR/Cas9 has proven to be highly efficient, as shown by the prominent loss of eye-pigmentation in the *oca2* crispants (Fig 1B

and Fig S1A), as well as in previous studies (Lischik et al. 2019; Hammouda et al. 2019). A similarly high penetrance was also observed in the *scn4ab* crispants, where we detected and quantified severe arrhythmia phenotypes such as AV-block with our assay (Fig 4, Movies S1 and S2). A 90 % prevalence of the arrhythmia phenotype and an absence of global phenotypes further reflect the specificity of this phenotype. Targeting some of the genes in our assays (e.g. *nkx2-5*, *smg6*, *naca*, *ttn.2*, *abcb4*) however, yielded a rather broad range of global developmental phenotypes, potentially reflecting their essential roles in embryonic development. To address this un-avoidable outcome when tackling genes with broader function (e.g. transcription factors or essential genes), we applied a developmental focusing filter in the analysis phase. Doing so, we avoid a biased assessment of the heart rate by ensuring the comparability of the embryo crispants on a global developmental scale, which in turn allows emphasizing cardiac-specific effects. Interestingly however, developmental focusing, although deemed important, in only few cases significantly altered the outcome of the analysis (Fig. S4). This reflects the robustness of the assay and the homogeneity of CRISPR/Cas9-induced phenotypes in the isogenic background of the medaka line used.

In a set of ten randomly chosen genes we observed a baseline occurrence of heart-affecting genes of about 20 % (Fig 2, and Fig S2). Relevantly, both genes

were implicated in heart functions, further reflecting the reliability of our model and approach. For *cdc42*, there is *a priori* evidence of its human orthologue in heart development as well as in regulating heart function across species (Qian et al. 2011; Li et al. 2017). Surprisingly, we did not find any associations (coding or non-coding) of *CDC42* to heart phenotypes in human GWAS according to the GRASP database (Eicher et al. 2015). As for *ogdh*, no experimental evidence in cardiac function has been previously reported, but a polymorphism located on one of its exons has been associated to heart phenotypes in human GWAS (Thanassoulis et al. 2013). Except for *duox*, which has been reported as having an indirect role in cardiac regeneration in zebrafish (Han et al. 2014), none of the other randomly selected genes were, to our knowledge, ever connected with cardiac function. In summary, from our random selection of genes, the only ones showing an effect (*ogdh* and *cdc42*) are connected to cardiac function by prior evidence. All but one positive (*HCN4*) controls among the hGWAS candidates resulted in a pronounced heart rate phenotype in our assay, reflecting their role in cardiac contraction (*TTN* and *NACA*), cardiac conduction and heart rate regulation (*CASQ2*, *KCNH2* and *SCN5A*) (Itoh-Satoh et al. 2002; Park et al. 2010; Faggioni & Knollmann 2012; Gianulis & Trudeau 2011; Zaklyazminskaya & Dzemeshkevich 2016; Huttner et al. 2013). For *hcn4*, we suspect compensation by the other medaka paralog *hcn4l*.

For eleven hGWAS candidate genes, our analysis provided the first experimental evidence validating a cardiac function. The identified genes represent new targets for future in-depth characterization and as candidates for predicting heart diseases prior to their onset. This is impressively substantiated by the emerging studies on the CCR4-NOT (*CNOT1*) complex in heart structure and function (Yamaguchi et al. 2018; Elmen et al. 2020).

Grouping the candidate genes according to their heart GWAS association into heart rate and non-heart rate-related phenotypes further exposed the prominent positive correlation between the associated human phenotype and the observed phenotype in medaka (Fig 3C).

Medaka's isogenic background, a product of inbreeding over multiple generations (Wittbrodt et al. 2002), enabled the detection of subtle changes in heart rate immediately in F0 crispants. This accelerated the analysis and avoided the necessity to analyze homozygous offspring in the second and third generation after CRISPR targeting.

It is noteworthy that despite the evolutionary distance from fish to humans the medaka phenotypes match the class of hGWAS effects. This is even more relevant since the roles of the genes in medaka were validated in embryos, suggesting that the validated marker genes have predictive power in humans. This deep functional conservation emphasizes the potential of our approach for

296 the identification and validation of novel predictive genetic markers for
297 cardiovascular diseases in humans. We have showcased a highly versatile,
298 sensitive and robust high-throughput reverse genetic validation assay to address
299 the pool of understudied, neglected putative candidates. In the future, the
300 combination of genetic validation and drug screening in a single platform
301 building on our assay will facilitate the simultaneous identification of novel
302 genetic players and interacting small molecules with rescuing power.
303
304 Materials and Methods
305 *Ethics Statement*
306 All fish are maintained in closed stocks at Heidelberg University. Medaka
307 (*Oryzias latipes*) husbandry (permit number 35–9185.64/BH Wittbrodt,
308 Regierungspräsidium Karlsruhe) was performed according to local animal
309 welfare standards (Tierschutzgesetz §11, Abs. 1, Nr. 1) in accordance with
310 European Union animal welfare guidelines (Bert et al., 2016). The fish facility is
311 under the supervision of the local representative of the animal welfare agency.
312 Medaka embryos of the wildtype Cab strain were used at stages prior to stage
313 42. Medaka were raised and maintained as described previously (Köster et al.,
314 1997).
315

316 *Candidate gene selection*

317 For the unbiased gene targeting, an online random number generator was used to
318 generate 10 numbers between 1 and 23622, corresponding to the number of
319 annotated medaka coding genes in Ensembl (Yates et al. 2020) (Table 1). The
320 number of exons for each gene was counted and a random number was
321 generated to select the exon for CRISPR/Cas9 targeting. For the targeted human
322 heart-GWAS (hGWAS) gene selection, the genome-wide repository of
323 associations between SNPs and phenotypes (GRASP v2.0) was used (Eicher et
324 al. 2015). In the search field, “Heart” and “Heart rate” were chosen as the
325 respective categories for all heart- and heart rate-related phenotypes associated
326 in human GWAS, only coding SNPs (i.e. SNP functional class = exons) were
327 searched for. List of resulting genes was extracted (Table 2), and candidate
328 genes for the functional validation assay were chosen. The focus was on
329 uncharacterized genes, or genes with no prior experimental link to heart
330 function, yet some known heart genes were included as proof of concept. For
331 each hGWAS candidate gene, the corresponding medaka ortholog was extracted
332 using Ensembl (Yates et al. 2020). For the few genes which did not have an
333 annotated medaka ortholog, the human protein sequence was BLASTed using
334 the “tblastn” function of the NCBI BLAST
335 (https://blast.ncbi.nlm.nih.gov/Blast.cgi) and Ensemble

(http://www.ensembl.org/Multi/Tools/Blast) online tools to obtain a target medaka locus. Using Geneious 8.1.9 (https://www.geneious.com), regions of interest (ROI) on medaka orthologous genes for CRISPR targeting were primarily chosen based on the corresponding location of human SNP when aligning the medaka and human protein sequences.

sgRNA target sites selection and in vitro transcription

All sgRNA target sites used in this study are listed in Table S1. sgRNAs were designed with CCTop as described in Stemmer et al. (Stemmer et al. 2015). sgRNA target sites were selected based on number of potential off-target sites and their corresponding mismatches. Preferably, sgRNAs selected had no off-target site or at least 3 nucleotide mismatches. sgRNAs for *oca2* were the same as in Lischik et al. (Lischik et al. 2019). Cloning of sgRNA templates and *in vitro* transcription was performed as detailed in Stemmer, et al. (Stemmer et al. 2015). All sgRNAs were initially tested after synthesis for *in vivo* targeting via injections into medaka embryos, followed by genotyping using our filter-in-tips protocol (Hammouda et al. 2019), in brief terms, by PCR amplification of target locus followed by T7 Endonuclease I assay (New England Biolabs).

Microinjection

Medaka one-cell stage embryos were injected in the cytoplasm as previously described (Stemmer et al. 2015). Injection solutions for CRISPR targeting comprised: 150 ng/µl *Cas9* mRNA, 15 ng/µl respective sgRNA and 10 ng/µl *GFP* mRNA as injection tracer. Control siblings were injected with of 10 ng/µl *GFP* mRNA only. Injected embryos were incubated at 28 °C in embryo rearing medium (ERM), screened for GFP expression at 1 dpf and transferred to methylene blue-containing ERM and incubated at 28 °C until analysis (4 dpf).

Sample preparation and Imaging

One day prior to imaging, medaka embryos were transferred from methylene blue-containing ERM into plain ERM and incubated at 28 °C. On day of imaging (4 dpf), individual medaka embryos (36 per sgRNA and 24 control injected) were administered to a 96 U-well microtiter plate (Nunc, Thermofisher #268152) containing 200 µl ERM per well and sealed using gas-permeable adhesive foil (4titude, Wotton, UK, 4ti-0516/96). Plates were automatically imaged using an ACQUIFER Imaging Machine (DITABIS AG, Pforzheim, Germany) at 21 and 28 °C with a 30-minute equilibration period before each measurement. Images were acquired in brightfield using 130 z-slices (dz = 0 µm) and a 2x Plan UW N.A. 0.06 objective (Nikon, Düsseldorf, Germany) to capture the centered embryo. Integration times were fixed with 80 % relative

white LED intensity and 10 ms exposure time. Therefore, the whole 96-well plate was captured, with image sequences (videos) of entire microwells of approx. 10 seconds with 13 frames per second (fps). More details can be found in Gierten, et al. (Gierten et al. 2020).

HeartBeat detection and data analysis

Image optimizations prior to analysis, as well as heart rate analysis using the *HeartBeat* software were performed as previously described (Gierten et al. 2020). In some instances, heart rates could not be scored due to inconvenient embryo orientations shielding the view of the heart. For *scn4ab* crispants with cardiac arrhythmias, atrium and ventricle for individual embryos were separately segmented, and the respective beating frequency for each chamber was measured. Data plots were generated using ggplot2 package (Wickham 2016) in R 3.6.1 (R Core Team, 2019) and R-studio 1.2.1335 (RStudio Team, 2018). Statistical analysis for heart rate comparisons were computed in R. Significant differences were determined by two-tailed Student's t-test. Significant *p*-values are indicated with asterisks (*) with $*p < 0.05$, $**p < 0.01$, $***p < 0.001$ and ns (not significant).

Embryo genotyping

Nucleic acid extraction and genotyping of embryos was done as previously described (Hammouda et al. 2019). Briefly, after imaging, embryos in 96-well plate were lysed in 50 µl Milli-Q water + 50 µl Fin-Clip lysis buffer each (0.4 M Tris-HCl pH 8.0, 5 mM EDTA pH 8.0, 0.15 M NaCl, 0.1 % SDS in Milli-Q water) using a custom 96-well mortar. The mortar was pre-cleaned by incubation in hypochlorite solution (1:10 dilution of commercial bleach reagent) for at least 15 minutes followed by 5 minutes incubation in Milli-Q water. Plates containing lysed embryos were stored at 4 °C until genotyping. To confirm CRISPR on-target activity, per experimental plate, 2 embryos per condition were chosen at random for genotyping by PCR amplification of target locus using our filter-in-tips approach (Hammouda et al. 2019), followed by T7 Endonuclease I Assay (New England Biolabs). 30 PCR cycles were run in all samples, all primers used for PCR are listed in Table S2. Annealing temperatures were calculated using the online NEB Tm calculator (https://tmcalculator.neb.com/).

Acknowledgments

We thank J. Gierten, V. Weinhardt, E. Tsingos and all members of the Wittbrodt lab for their critical, constructive feedback on the procedure and the manuscript, F. Loosli and S. Lemke for their constructive feedback towards the project as

well as J. Backs and E. Furlong for an outside perspective. We thank T. Kellner for excellent technical support. We acknowledge the excellent fish husbandry of E. Leist, M. Majewsky and A. Saraceno. We thank J. Gehrig (ACQUIFER Imaging GmbH) for supporting us with the Imaging machine. This research was funded through DFG CRC-1324 TP B4 and NIH 5R01ES029917 – 03, KiyosuTox. O.T.H. is a member of the Heidelberg Biosciences International Graduate School (HBIGS) and was supported by a fellowship of the Deutsches Zentrum für Herz-Kreislauf-Forschung (DZHK).

Author contributions

O.T.H., T.T. and J.W. designed the study and implemented the methodology. O.T.H., V.K. and M.Y.W. synthesized the guides. O.T.H. performed experiments. O.T.H. analyzed the data with contributions by M.Y.W. and V.K.. O.T.H. visualized data. O.T.H. and J.W. wrote the first draft of the manuscript. O.T.H., T.T., and J.W. finalized the manuscript. J.W. provided resources and supervised this work.

Conflict of interest

All authors declare no competing interests.

436 References

437 Beere, P.A., Glagov, S. & Zarins, C.K., 1984. Retarding effect of lowered heart
438 rate on coronary atherosclerosis. *Science*, 226(4671), p.180.

439 Benson, M.A. et al., 2017. Ryanodine receptors are part of the myospryn
440 complex in cardiac muscle. *Scientific Reports*, pp.1–12.

441 Bert, B. et al., 2016. Considerations for a European animal welfare standard to
442 evaluate adverse phenotypes in teleost fish. *The EMBO Journal*, 35(11),
443 pp.1151–1154.

444 Cambien, F. & Tiret, L., 2007. Genetics of Cardiovascular Diseases.
445 *Circulation*, 116(15), pp.1714–1724.

446 Cordell, H.J. et al., 2013. Genome-wide association study identifies loci on
447 12q24 and 13q32 associated with Tetralogy of Fallot. *Human Molecular*
448 *Genetics*, 22(7), pp.1473–1481.

449 DYER, A.R. et al., 1980. HEART RATE AS A PROGNOSTIC FACTOR FOR
450 CORONARY HEART DISEASE AND MORTALITY: FINDINGS IN
451 THREE CHICAGO EPIDEMIOLOGIC STUDIES. *American Journal of*
452 *Epidemiology*, 112(6), pp.736–749.

453 Eicher, J.D. et al., 2015. GRASP v2.0: an update on the Genome-Wide
454 Repository of Associations between SNPs and phenotypes. *Nucleic Acids*
455 *Research*, 43(D1), pp.D799–D804.

456 Eijgelsheim, M. et al., 2010. Genome-wide association analysis identifies
457 multiple loci related to resting heart rate. *Human Molecular Genetics*,
458 19(19), pp.3885–3894.

459 Elmen, L. et al., 2020. Silencing of CCR4-NOT complex subunits affect heart
460 structure and function. *Disease Models & Mechanisms*, pp.dmm.044727–33.

461 Eppinga, R.N. et al., 2016. Identification of genomic loci associated with resting
462 heart rate and shared genetic predictors with all-cause mortality. *Nature*
463 *Genetics*, 48(12), pp.1557–1563.

464 Faggioni, M. & Knollmann, B.C., 2012. Calsequestrin 2 and arrhythmias.
465 *American Journal of Physiology-Heart and Circulatory Physiology*, 302(6),
466 pp.H1250–H1260.

467 Fukamachi, S. et al., 2004. Conserved function of medaka pink-eyed dilution in
468 melanin synthesis and its divergent transcriptional regulation in gonads
469 among vertebrates. *Genetics*, 168(3), pp.1519–1527.

470 Gianulis, E.C. & Trudeau, M.C., 2011. Rescue of Aberrant Gating by a
471 Genetically Encoded PAS (Per-Arnt-Sim) Domain in Several Long QT
472 Syndrome Mutant Human Ether-á-go-go-related Gene Potassium Channels.
473 *Journal of Biological Chemistry*, 286(25), pp.22160–22169.

474 Gierten, J. et al., 2020. Automated high-throughput heartbeat quantification in
475 medaka and zebrafish embryos under physiological conditions. *Scientific*
476 *Reports*, pp.1–12.

477 Gillum, R.F., Makuc, D.M. & Feldman, J.J., 1991. Pulse rate, coronary heart
478 disease, and death: The NHANES I Epidemiologic Follow-up Study.
479 *American Heart Journal*, 121(1), pp.172–177.

480 Gut, P. et al., 2017. Little Fish, Big Data: Zebrafish as a Model for
481 Cardiovascular and Metabolic Disease. *Physiological Reviews*, 97(3),
482 pp.889–938.

483 Hammouda, O.T. et al., 2019. Swift Large-scale Examination of Directed
484 Genome Editing S. C. F. Neuhauss, ed. *PLoS ONE*, 14(3), pp.e0213317–11.

485 Han, P. et al., 2014. Hydrogen peroxide primes heart regeneration with a
486 derepression mechanism. *Nature Publishing Group*, pp.1–17.

487 Heyde, von der, B. et al., 2020. Translating GWAS-identified loci for cardiac
488 rhythm and rate using an in vivo image- and CRISPR/Cas9-based approach.
489 *Scientific Reports*, pp.1–18.

490 Hiura, Y. et al., 2010. A Genome-Wide Association Study of Hypertension-
491 Related Phenotypes in a Japanese Population. *Circulation Journal*, 74(11),
492 pp.2353–2359.

493 Hoed, den, M. et al., 2013. Identification of heart rate–associated loci and their
494 effects on cardiac conduction and rhythm disorders. *Nature Genetics*, pp.1–
495 14.

496 Holm, H. et al., 2011. A rare variant in MYH6 is associated with high risk of
497 sick sinus syndrome. *Nature Genetics*, 43(4), pp.316–320.

Hu, Z. et al., 2013. A genome-wide association study identifies two risk loci for congenital heart malformations in Han Chinese populations. *Nature Genetics*, pp.1–5.

Huttner, I.G. et al., 2013. A transgenic zebrafish model of a human cardiac sodium channel mutation exhibits bradycardia, conduction-system abnormalities and early death. *Journal of Molecular and Cellular Cardiology*, 61(C), pp.123–132.

Ikram, M.A. et al., 2009. Genomewide Association Studies of Stroke. *New England Journal of Medicine*, 360(17), pp.1718–1728.

Itoh-Satoh, M. et al., 2002. Titin Mutations as the Molecular Basis for Dilated Cardiomyopathy. *Biochemical and Biophysical Research Communications*, 291(2), pp.385–393.

Iwamatsu, T., 2004. Stages of normal development in the medaka Oryzias latipes. *Mechanisms of Development*, 121(7-8), pp.605–618.

Kathiresan, S. & Srivastava, D., 2012. Genetics of Human Cardiovascular Disease. *Cell*, 148(6), pp.1242–1257.

Koster, R. et al., 1997. Medaka spalt acts as a target gene of hedgehog signaling. *Development*, 124(16), p.3147.

Lessman, C.A., 2011. The developing zebrafish (Danio rerio): A vertebrate model for high-throughput screening of chemical libraries R. S. Tuan, ed. *Birth Defects Research Part C: Embryo Today: Reviews*, 93(3), pp.268–280.

Li, J. et al., 2017. Essential role of Cdc42 in cardiomyocyte proliferation and cell-cell adhesion during heart development. *Developmental Biology*, 421(2), pp.271–283.

Lischik, C.Q., Adelmann, L. & Wittbrodt, J., 2019. Enhanced in vivo-imaging in medaka by optimized anaesthesia, fluorescent protein selection and removal of pigmentation C. Winkler, ed. *PLoS ONE*, 14(3), pp.e0212956–19.

Marroni, F. et al., 2009. A Genome-Wide Association Scan of RR and QT Interval Duration in 3 European Genetically Isolated Populations. *Circulation: Cardiovascular Genetics*, 2(4), pp.322–328.

528 Matsa, L.S. et al., 2014. Endothelin 1 gene as a modifier in dilated
529 cardiomyopathy. *Gene*, 548(2), pp.256–262.

530 McGill, H.C., Jr, McMahan, C.A. & Gidding, S.S., 2008. Preventing Heart
531 Disease in the 21st Century. *Circulation*, 117(9), pp.1216–1227.

532 MD, P.M.B. et al., 2010. Heart rate as a risk factor in chronic heart failure
533 (SHIFT): the association between heart rate and outcomes in a randomised
534 placebo-controlled trial. *The Lancet*, 376(9744), pp.886–894.

535 Meyer, H.V. et al., 2020. Genetic and functional insights into the fractal
536 structure of the heart. *Nature*, pp.1–25.

537 Nemtsas, P. et al., 2010. Adult zebrafish heart as a model for human heart? An
538 electrophysiological study. *Journal of Molecular and Cellular Cardiology*,
539 48(1), pp.161–171.

540 Newton-Cheh, C. et al., 2009. Common variants at ten loci influence QT
541 interval duration in the QTGEN Study. *Nature Genetics*, 41(4), pp.399–406.

542 Oxendine, S.L. et al., 2006. Adapting the medaka embryo assay to a high-
543 throughput approach for developmental toxicity testing. *NeuroToxicology*,
544 27(5), pp.840–845.

545 Paré, G. et al., 2013. Genetic Determinants of Dabigatran Plasma Levels and
546 Their Relation to Bleeding. *Circulation*, 127(13), pp.1404–1412.

547 Park, C.Y. et al., 2010. skNAC, a Smyd1-interacting transcription factor, is
548 involved in cardiac development and skeletal muscle growth and
549 regeneration. *Proc Natl Acad Sci USA*, 107(48), p.20750.

550 Pfeufer, A. et al., 2009. Common variants at ten loci modulate the QT interval
551 duration in the QTSCD Study. *Nature Genetics*, 41(4), pp.407–414.

552 Qian, L. et al., 2011. Tinman/Nkx2-5 acts via miR-1 and upstream of Cdc42 to
553 regulate heart function across species. *The Journal of Cell Biology*, 193(7),
554 pp.1181–1196.

555 R Core Team (2019). R: A language and environment for statistical computing.
556 R Foundation for Statistical Computing, Vienna, Austria. URL
557 https://www.R-project.org/

Rathjens, F.S. et al., 2020. Preclinical evidence for the therapeutic value of TBX5 normalization in arrhythmia control. *Cardiovascular Research*.

Ritchie, M.D. et al., 2013. Genome- and Phenome-Wide Analyses of Cardiac Conduction Identifies Markers of Arrhythmia Risk. *Circulation*, 127(13), pp.1377–1385.

RStudio Team (2018). RStudio: Integrated Development for R. RStudio, Inc., Boston, MA URL http://www.rstudio.com/

Shankaran, S.S. et al., 2018. CRISPR/Cas9-Directed Gene Editing for the Generation of Loss-of-Function Mutants in High-Throughput Zebrafish F 0Screens. *Current Protocols in Molecular Biology*, 119(1), pp.4257–22.

Smith, J.G. et al., 2009. Genome-wide association study of electrocardiographic conduction measures in an isolated founder population: Kosrae. *HRTHM*, 6(5), pp.634–641.

Sotoodehnia, N. et al., 2010. Common variants in 22 loci are associated with QRS duration and cardiac ventricular conduction. *Nature Genetics*, pp.1–11.

Stemmer, M. et al., 2015. CCTop: An Intuitive, Flexible and Reliable CRISPR/Cas9 Target Prediction Tool S. Maas, ed. *PLoS ONE*, 10(4), pp.e0124633–11.

Targoff, K.L. et al., 2013. Nkx genes are essential for maintenance of ventricular identity. *Development*, 140(20), pp.4203–4213.

Teboul, L., 2017. Phenotyping first-generation genome editing mutants: a new standard? *Mammalian Genome*, 28(7), pp.377–382.

Thanassoulis, G. et al., 2013. Genetic Associations with Valvular Calcification and Aortic Stenosis. *New England Journal of Medicine*, 368(6), pp.503–512.

Vasan, R.S. et al., 2009. Genetic Variants Associated With Cardiac Structure and Function: A Meta-analysis and Replication of Genome-wide Association Data. *JAMA*, 302(2), pp.168–178.

Villard, E. et al., 2011. A genome-wide association study identifies two loci associated with heart failure due to dilated cardiomyopathy. *European Heart Journal*, 32(9), pp.1065–1076.

588 Wickham, H., 2016. *ggplot2: Elegant Graphics for Data Analysis*, Springer-
589 Verlag New York. Available at: https://ggplot2.tidyverse.org.

590 Wittbrodt, J., Shima, A. & Schartl, M., 2002. MEDAKA — A MODEL
591 ORGANISM FROM THE FAR EAST. *Nature Reviews Genetics*, 3(1),
592 pp.53–64.

593 Wooten, E.C. et al., 2010. Application of Gene Network Analysis Techniques
594 Identifies AXIN1/PDIA2 and Endoglin Haplotypes Associated with
595 Bicuspid Aortic Valve A. E. Toland, ed. *PLoS ONE*, 5(1), pp.e8830–10.

596 Wu, R.S. et al., 2018. A Rapid Method for Directed Gene Knockout for
597 Screening in G0 Zebrafish. *Developmental Cell*, 46(1), pp.112–125.e4.

598 Yamaguchi, T. et al., 2018. The CCR4-NOT deadenylase complex controls
599 Atg7-dependent cell death and heart function. *Sci. Signal.*, 11(516),
600 p.eaan3638.

601 Yates, A.D. et al., 2020. Ensembl 2020. *Nucleic Acids Research*, 48(D1),
602 pp.D682–D688.

603 Yonekura, M. et al., 2018. Medaka as a model for ECG analysis and the effect
604 of verapamil. *Journal of Pharmacological Science*, 137(1), pp.55–60.

605 Zakariyah, A.F. et al., 2017. Congenital heart defect causing mutation in Nkx2.5
606 displays in vivo functional deficit. *Journal of Molecular and Cellular*
607 *Cardiology*, 105(C), pp.89–98.

608 Zaklyazminskaya, E. & Dzemeshkevich, S., 2016. The role of mutations in the
609 SCN5A gene in cardiomyopathies. *BBA - Molecular Cell Research*,
610 1863(Part B), pp.1799–1805.

611

612 Main Figure Legends

613 Figure 1 - Medaka *nkx2-5* embryo crispants show heart rate phenotypes

614 **A** Schematic overview of functional gene validation pipeline: position of human

615 coding SNP mapped to medaka orthologous gene to define region of interest for

616 CRISPR/Cas9 gene targeting (double strand break; DSB). 96-well plate layout
617 of embryo crispants (Target Gene 1 and 2) separated by *GFP* mRNA mock-
618 injected siblings. Embryos are subjected to high-throughput imaging followed
619 by automated heart detection (blue area) and heart rate quantification (graphical
620 output; *HeartBeat* software (Gierten et al. 2020).
621 **B** Comparison of the atrium (A, dotted red line) and ventricle (V, dotted yellow
622 line) in *GFP*-injected (mock) and *nkx2-5* and *oca2* crispant embryos (stage 40).
623 Note: *nkx2-5* crispant shows dilated heart chambers while mock injected and
624 *oca2* crispant embryos are indistinguishable. Loss of eye pigmentation in *oca2*
625 crispants reflects high efficiency of knock-out rate in the injected generation.
626 **C** Heart rate measurements (beats per minute, bpm) of *GFP*-injected (mock;
627 dark grey), *nkx2-5* and *oca2* embryo crispants (4 dpf) at 21 and 28°C, before
628 (left) and after (right) exclusion of severely affected embryos (developmental
629 focusing) reveal elevation of mean heart rates in *nkx2-5* targeted embryos,
630 significant at 21°C (red). Significance was determined by two-tailed Student's t-
631 test; *$p < 0.05$, **$p < 0.01$, ns (not significant; light grey). For biological
632 replicates see Source Data Fig 1C.
633
634 Figure 2 - Baseline probability of heart rate phenotype assessed via *in vivo*
635 targeting of randomly selected genes

636 **A** Heart rate measurements (beats per minute, bpm) of *GFP*-injected (mock) and
637 corresponding sibling embryo crispants at 21 and 28°C after developmental
638 focusing. Different experimental plates are represented by breaks on the x-axis.
639 Significant differences in mean heart rates were determined between each
640 embryo crispant group and its corresponding sibling control group by two-tailed
641 Student's t-test; *$p < 0.05$, ***$p < 0.001$, ns (not significant). Crispants showing
642 significant heart rate phenotype (red), *GFP*-injected controls (mock; dark grey),
643 crispants showing no significant heart rate phenotype (light grey).
644 **B** Heatmap quantitative representation of the data shown in (A); for each
645 measured temperature, the percent change in mean heart rate (HR % Change)
646 between crispants and their corresponding control sibling, flanked by the
647 statistical significance (*p*-value) of the observed change calculated by two-tailed
648 Student's t-test on the full distribution in (A). Genes showing significant heart
649 rate phenotypes are indicated in bold. For biological replicates see Source Data
650 Fig S2.
651
652 Figure 3 - Targeted human heart-GWAS validations reveal new genes affecting
653 heart rate
654 **A** Heatmap quantitative representation of the comparative heart rate analysis
655 between each embryo crispant group and its corresponding control sibling group

after developmental focusing (also see plots in Fig S3); for each measured temperature, the percent change in mean heart rate (HR % Change) between crispants and their corresponding control sibling, flanked by the statistical significance (*p*-value) of the observed change calculated by two-tailed Student's t-test on the full distribution (Fig S3). Genes showing significant heart rate phenotypes are indicated in bold. For biological replicates see Source Data Fig S3.

B Venn diagram summarizing the genes with significantly different heart rate (HR) phenotypes only at 21°C, only at 28°C or at both temperatures (dark grey).

C Stacked plots representing percentage of genes showing a significant heart rate phenotype (dark grey) in each group. Number of genes for each group is denoted (n). hGWAS corresponds to the selection of genes associated to heart phenotypes in human GWAS.

Figure 4 - AV-block type arrhythmia in medaka *scn4ab* embryo crispants

A Heart rate measurements (beats per minute, bpm) of *GFP*-injected (mock; dark grey) and *scn4ab* crispant (red) embryos at 21 and 28°C; note the bimodal distribution in *scn4ab* crispants.

B Paired plots showing heart rate scores for each chamber separately (atrium in blue; ventricle in red) in individual embryos at both temperatures.

676

677 Tables and their legends

678 *Table 1. List of randomly selected genes*

679 Medaka Ensembl gene names and codes, as well as orthologous human genes as

680 annotated in the 95th Ensembl release.

681

682 *Table 2. List of candidate genes extracted from Human GWAS using GRASP 2.0*

683 *Database*

684 Human genes are categorized according to their association into “heart rate”

685 (bold) and “non-heart rate” (non-bold) related phenotypes in human GWAS.

686

687 *Table S1. List of sgRNAs used*

688 sgRNA target sites given in 5’-3’ direction, protospacer adjacent motif (PAM)

689 in square brackets.

690

691 *Table S2. List of primers used for genotyping by PCR*

692 Source Data Fig 1C. Biological replicates for Fig 1C

693 Source Data Fig S1. Biological replicates for Fig S1 B-C

694 Source Data Fig S2. Biological replicates for Fig 2 and S2

695 Source Data Fig S3. Biological replicates for Fig 3A, S3 and S4

696

697 Supplementary Figure legends

698 Figure S1: Consistent heart rate phenotype observed in medaka *nkx2-5* crispants

699 **A** Overview of 96-well plate with embryos injected with sgRNA against *nkx2-5*

700 or *oca2*, as well as embryos mock injected with *gfp mRNA* (Fig 1C). Note the

701 loss of eye pigmentation in *oca2* crispant embryos.

702 **B-C** Heart rate measurements of *GFP*-injected (mock; dark grey) and *nkx2-5*

703 embryo crispants (**B:** second replicate of *nxk2-5_T4*; **C:** different sgRNA *nkx2-*

704 *5_T5* targeting same region of interest) at 21 and 28°C, before and after

705 exclusion of severely affected embryos (< stage 28; developmental focusing).

706 Significant differences are shown in red and were determined by two-tailed

707 Student's t-test; *$p < 0.05$, **$p < 0.01$, ns (not significant; light grey). For

708 biological replicates see Source Data Fig S1.

709

710 Figure S2: Developmental focusing does not alter analysis outcome of random

711 gene selection

712 Heatmap quantitative representation of the comparative heart rate analysis

713 between each embryo crispant group and its corresponding control sibling group

714 before and after developmental focusing; for each measured temperature, the

715 percent change in mean heart rate (HR % Change) between crispants and their

716 corresponding control sibling, flanked by the statistical significance (*p*-value) of
717 the observed change calculated by two-tailed Student's t-test on the full
718 distribution. Genes showing significant heart rate phenotypes are indicated in
719 bold. For biological replicates see Source Data Fig S2.
720
721 Figure S3: Comparative analysis of mean heart rates in targeted hGWAS gene
722 selection
723 Heart rate measurements (beats per minute, bpm) of *GFP*-injected (mock; dark
724 grey) and corresponding sibling embryo crispants at 21 and 28°C after
725 developmental focusing (also see heatmap representation of the data in Fig 3A).
726 Different experimental plates are represented by breaks on the x-axis.
727 Significant differences in mean heart rates were determined between each
728 embryo crispant group and its corresponding sibling control group by two-tailed
729 Student's t-test; $*p < 0.05$, $**p < 0.01$, $***p < 0.001$, ns (not significant). Red
730 groups correspond to crispants showing significant heart rate phenotypes, and
731 light grey groups correspond to crispants showing no significant heart rate
732 phenotype. For biological replicates see Source Data Fig S3.
733
734 Fig S4: Developmental focusing does not alter analysis outcome of targeted
735 hGWAS genes

736 Heatmap quantitative representation of the comparative heart rate analysis
737 between each embryo crispant group and its corresponding control sibling group
738 before and after developmental focusing; for each measured temperature, the
739 percent change in mean heart rate (HR % Change) between crispants and their
740 corresponding control siblings, flanked by the statistical significance (*p*-value)
741 of the observed change, calculated by two-tailed Student's t-test on the full
742 distribution. Genes showing significantly different heart rate phenotypes are
743 indicated in bold. For biological replicates see Source Data Fig S3.
744
745 Movie S1: Moderate AV-block arrhythmia observed in medaka *scn4ab* crispants
746 Side by side comparison of rhythmic heartbeat of *GFP*-injected (mock; left) and
747 arrhythmic *scn4ab* crispants displaying 2:1 AV-block phenotype (right). Videos
748 of medaka embryos (stage 36) were acquired using a stereomicroscope under
749 bright field illumination.
750
751 Movie S2: Severe AV-block arrhythmia observed in medaka *scn4ab* crispants
752 Side by side comparison of rhythmic heartbeat of *GFP*-injected (mock; left) and
753 arrhythmic *scn4ab* crispants displaying severe AV-block phenotype (right).
754 Videos of medaka embryos (stage 40) were acquired using a stereomicroscope
755 under bright field illumination.

Hammouda et al. Figure 1

A

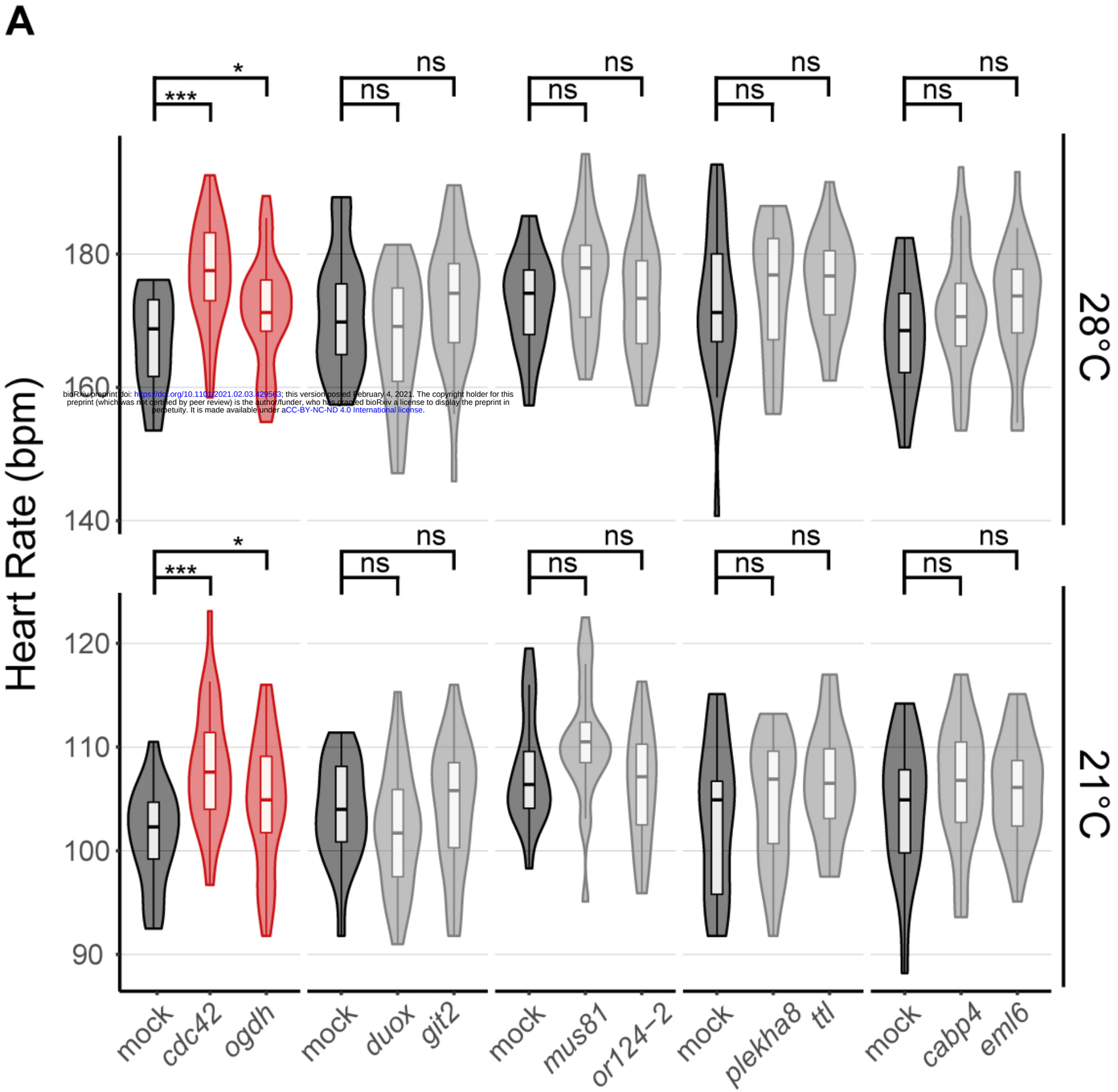

B

	21°C HR % Change	21°C *p*-value	28°C HR % Change	28°C *p*-value
cdc42	6.4	5.9e−05	6.3	2.0e−05
ogdh	3.2	3.4e−02	2.8	4.0e−02
duox	−1.6	2.9e−01	−2.2	1.7e−01
git2	0.5	7.2e−01	0.9	5.8e−01
mus81	2.7	1.1e−01	2.3	8.3e−02
or124-2	−1.3	3.9e−01	0.0	9.9e−01
plekha8	1.3	4.9e−01	0.8	6.7e−01
ttl	3.2	8.3e−02	1.7	3.1e−01
cabp4	2.0	2.3e−01	1.9	1.9e−01
eml6	1.6	3.2e−01	2.7	7.4e−02

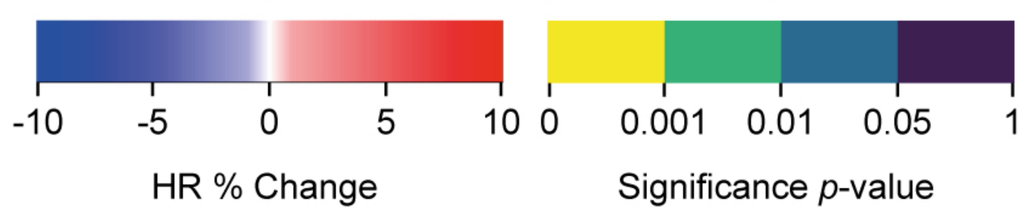

Hammouda et al. Figure 2

A

21°C HR % Change	21°C *p*-value		28°C HR % Change	28°C *p*-value
4.3	2.0e−02	***naca***	6.2	1.0e−05
7.1	1.3e−04	***myrf***	6.8	1.3e−04
6.5	1.9e−05	***casq2***	5.1	4.6e−04
3.3	2.9e−02	***trappc12***	5.2	4.7e−04
−12.3	7.1e−04	***scn4ab***	−15.2	5.7e−04
3.9	9.6e−02	***padi2***	7.1	8.3e−04
4.5	6.6e−03	***kcnh2***	5.2	1.5e−03
2.1	1.6e−01	***smg6***	3.4	9.7e−03
−1.6	2.4e−01	***sspo***	−2.9	1.3e−02
4.5	5.2e−03	***ttn.2***	2.7	2.5e−02
3.0	7.8e−02	***cmya5***	3.1	3.0e−02
6.4	9.0e−06	***ccdc141***	0.8	5.2e−01
3.3	7.4e−03	***gigyf1***	−0.5	6.9e−01
4.4	9.8e−03	***cnot1***	2.2	2.1e−01
2.9	2.9e−02	***homeza***	0.5	7.2e−01
2.4	4.9e−02	***slc17a3***	−1.4	3.4e−01
3.0	6.2e−02	*rnf207b*	2.3	6.4e−02
0.4	8.5e−01	*atp8b4*	3.6	8.1e−02
−0.9	5.6e−01	*hcn4*	−2.3	1.0e−01
1.4	3.5e−01	*ppp1r9a*	2.5	1.4e−01
0.3	8.5e−01	*zfhx3*	−1.9	1.7e−01
−0.4	8.1e−01	*or5au1*	−1.7	1.9e−01
2.3	6.3e−02	*scmh1*	1.9	2.4e−01
4.4	1.3e−01	*grid2*	2.6	2.7e−01
0.7	6.7e−01	*piezo1*	1.2	3.1e−01
−2.1	1.6e−01	*veph1*	−1.5	3.2e−01
0.5	7.6e−01	*clcnk*	−1.2	3.8e−01
2.4	1.3e−01	*mlnar1*	1.2	4.4e−01
1.8	2.4e−01	*bag3*	−0.9	4.9e−01
1.6	3.6e−01	*abcb4*	1.1	4.9e−01
−0.6	7.0e−01	*cep85l*	0.8	5.2e−01
−1.7	2.6e−01	*edn1*	−0.7	5.6e−01
0.7	6.3e−01	*plg*	0.8	5.7e−01
−0.5	7.6e−01	*nubp2*	−0.8	5.9e−01
0.7	6.7e−01	*col9a1b*	0.7	6.0e−01
−1.3	3.7e−01	*rgs3a*	−0.2	9.0e−01
2.1	1.7e−01	*maml3*	−0.1	9.2e−01
1.6	2.1e−01	*xylb*	−0.1	9.3e−01
0.4	8.0e−01	*sh2b3*	−0.1	9.4e−01
−0.1	9.4e−01	*ufsp1*	−0.1	9.6e−01

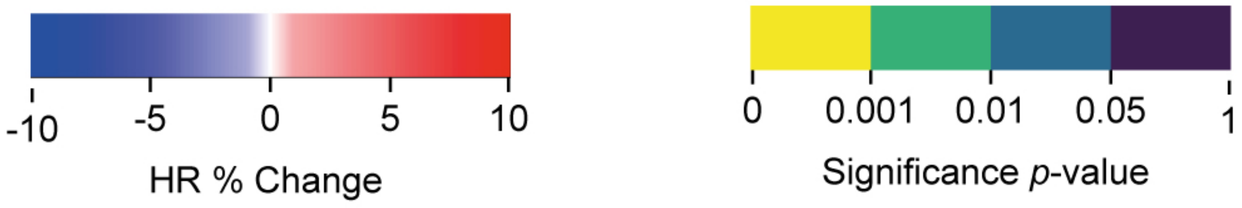

B

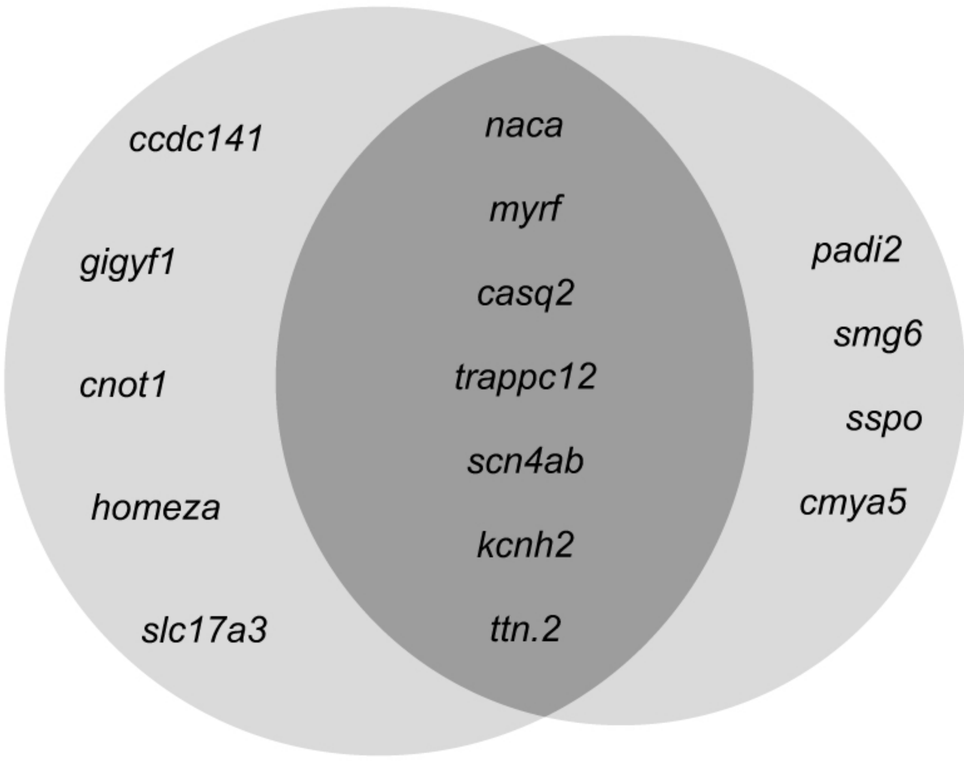

C

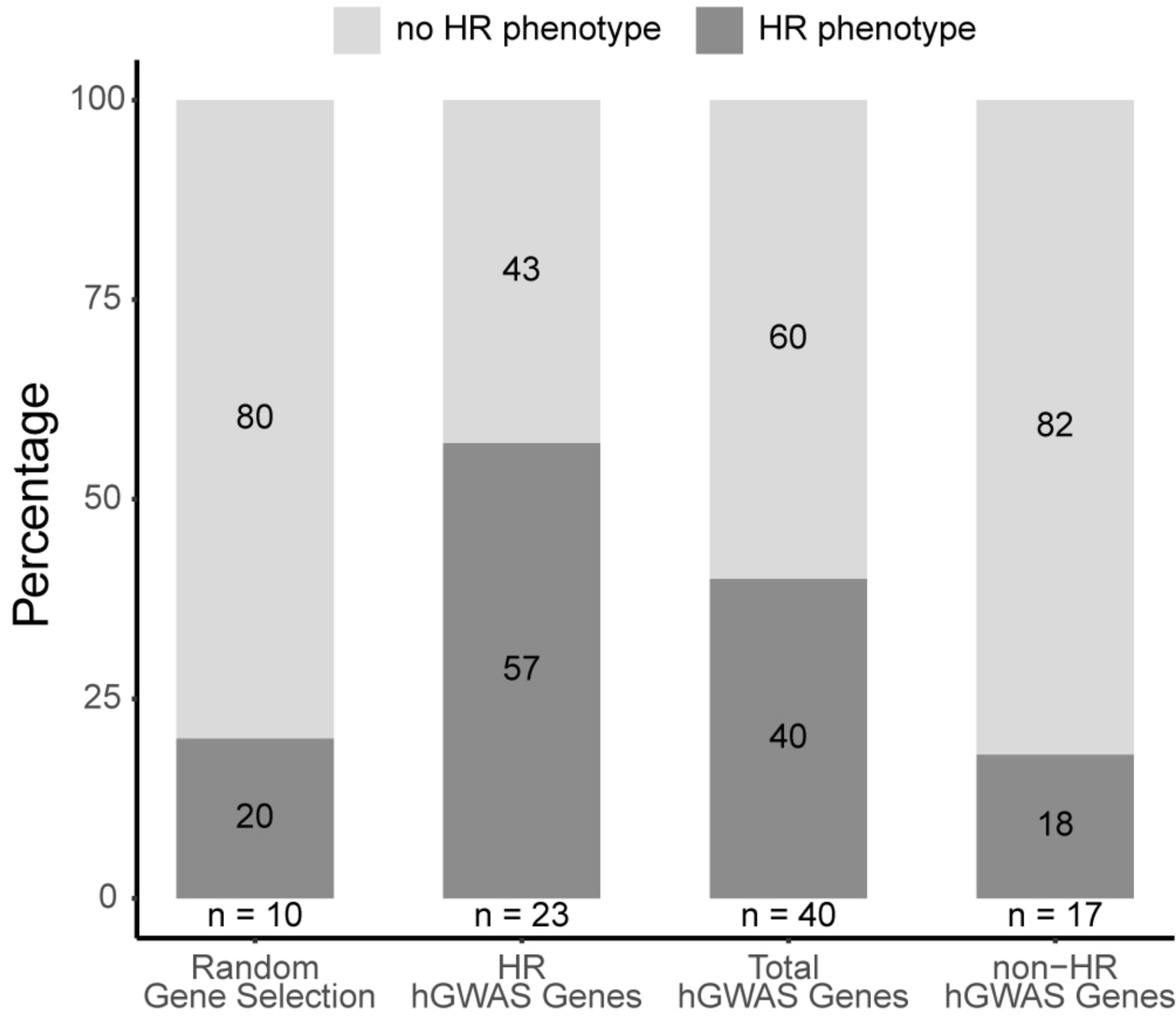

Hammouda et al. Figure 3

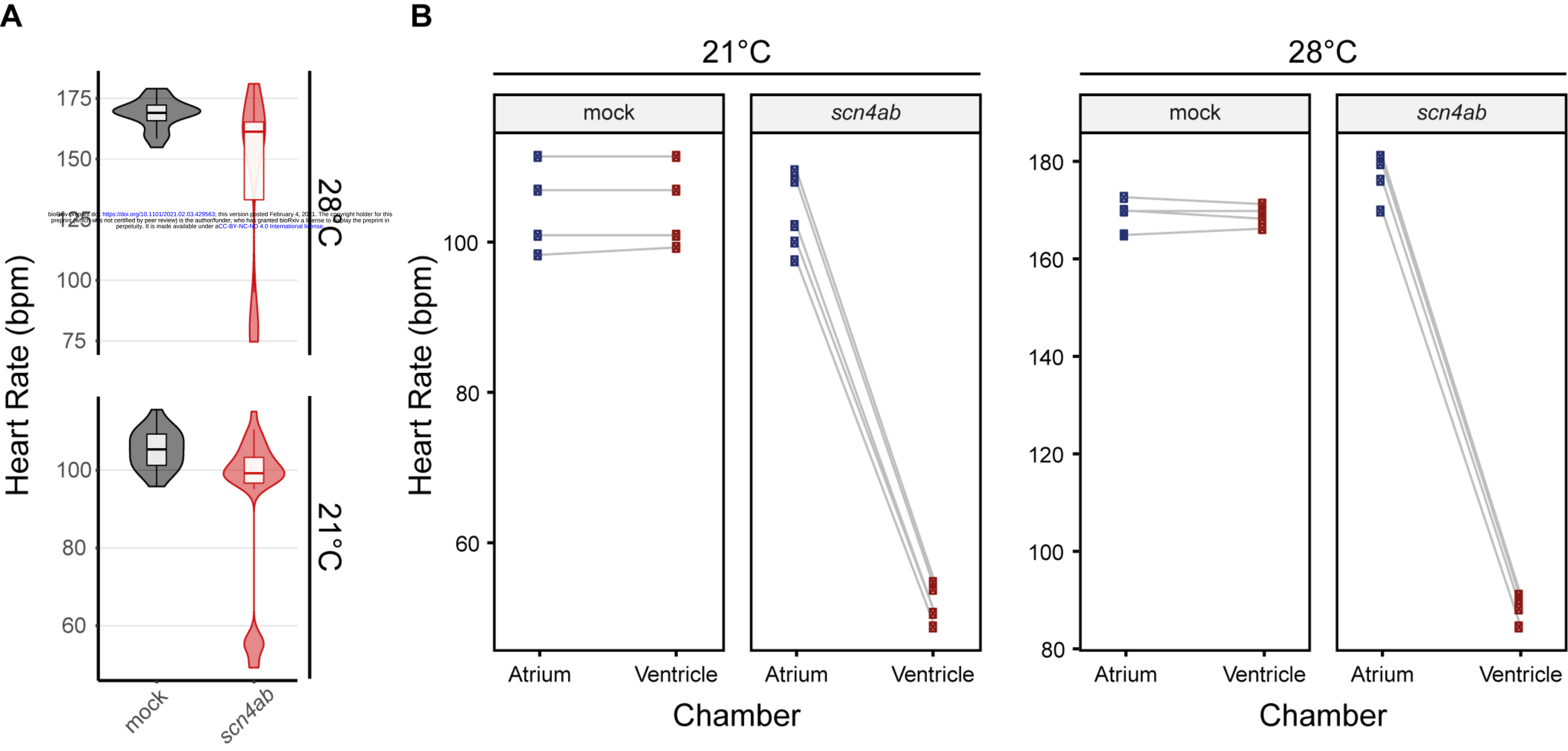

Hammouda et al. Figure 4

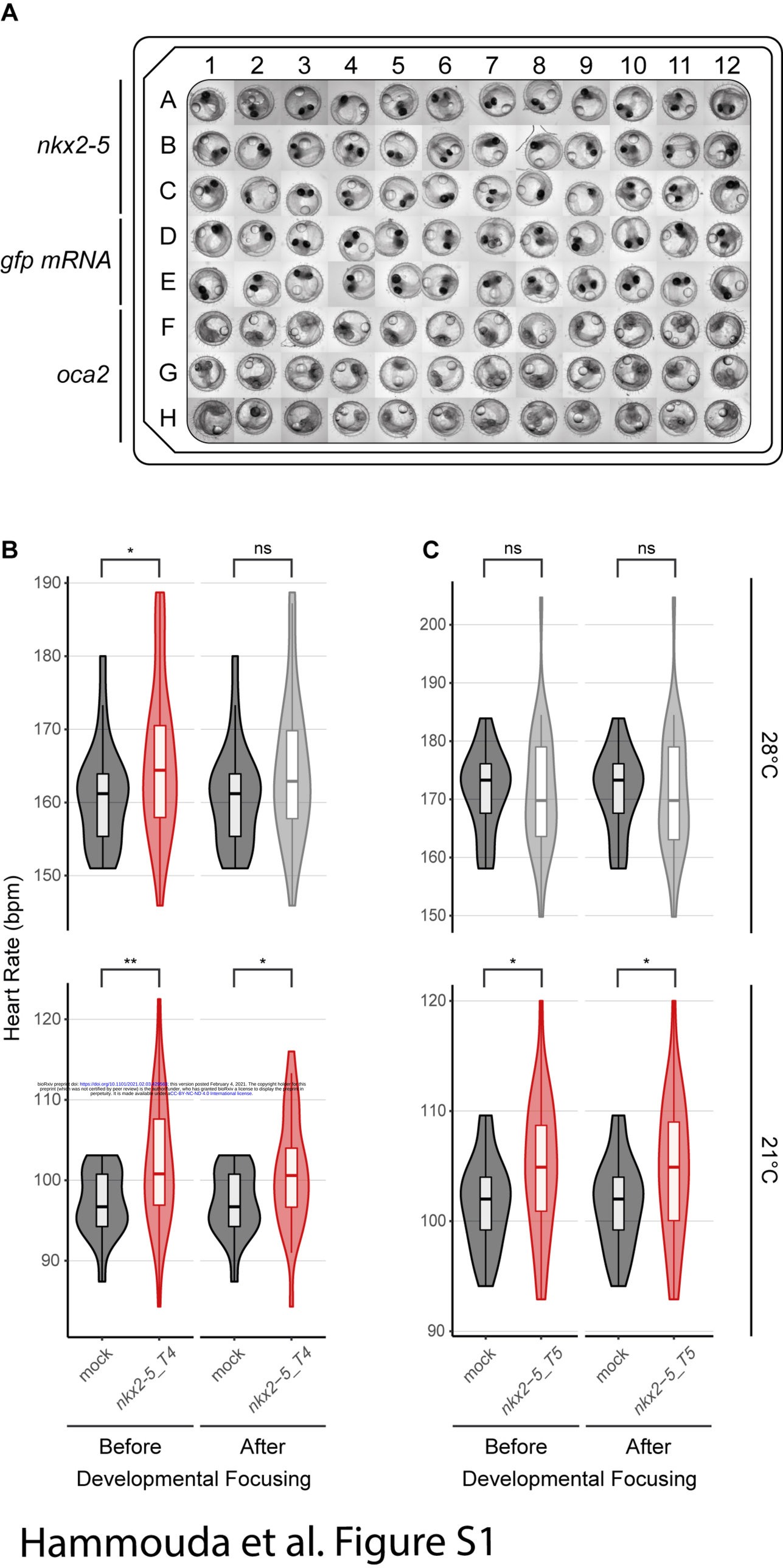

Hammouda et al. Figure S1

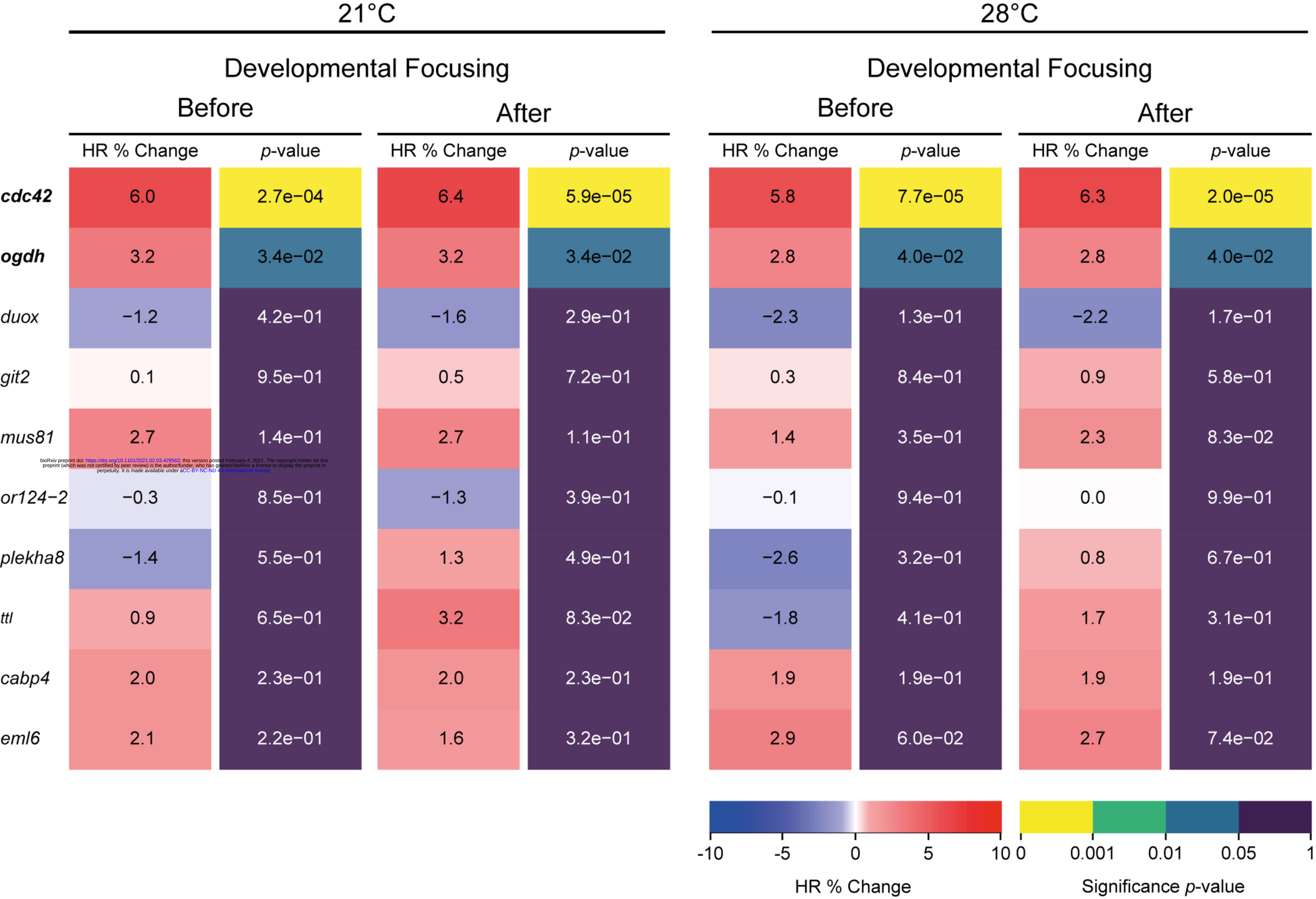

Hammouda et al. Figure S2

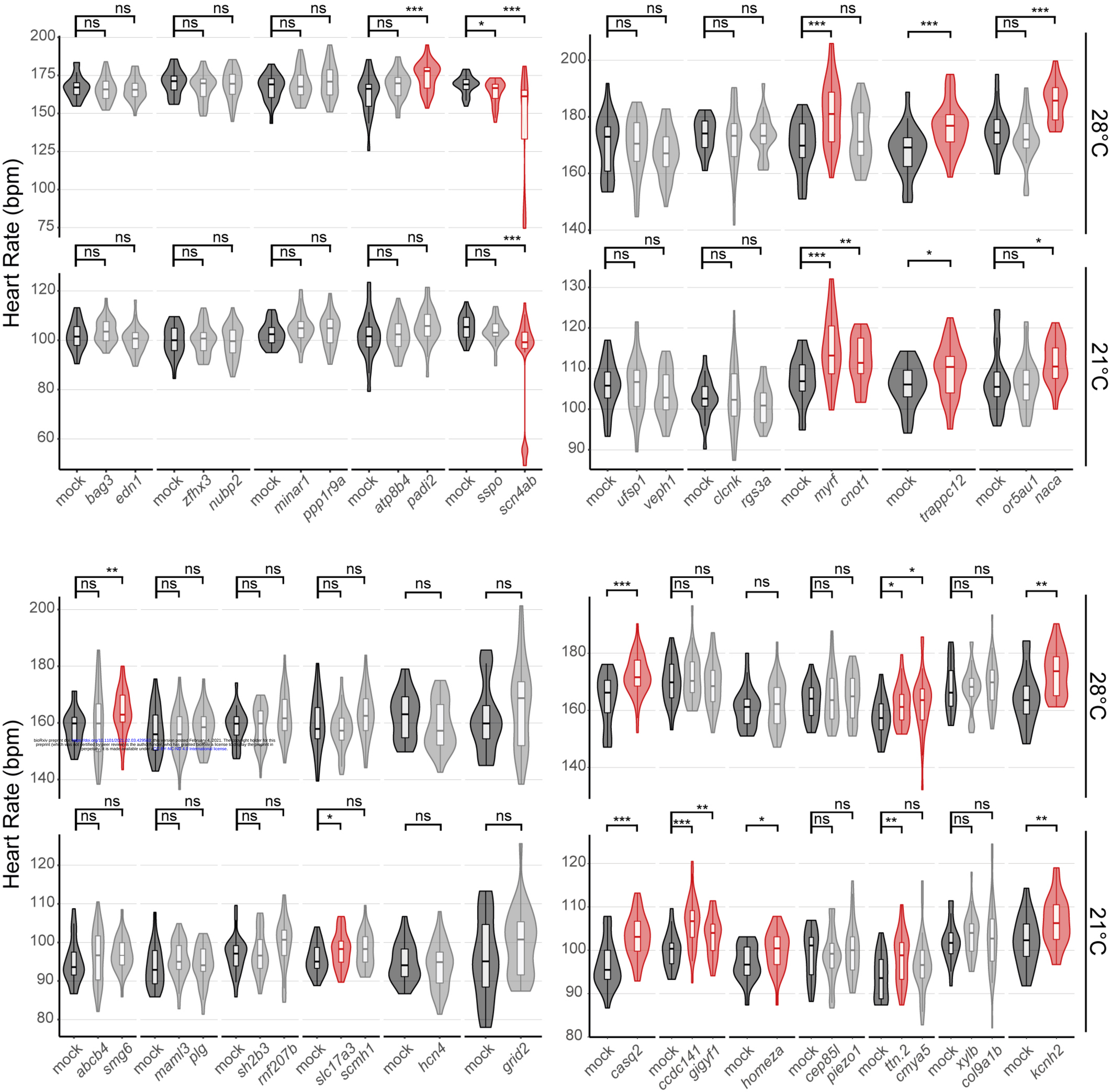

Hammouda et al. Figure S3

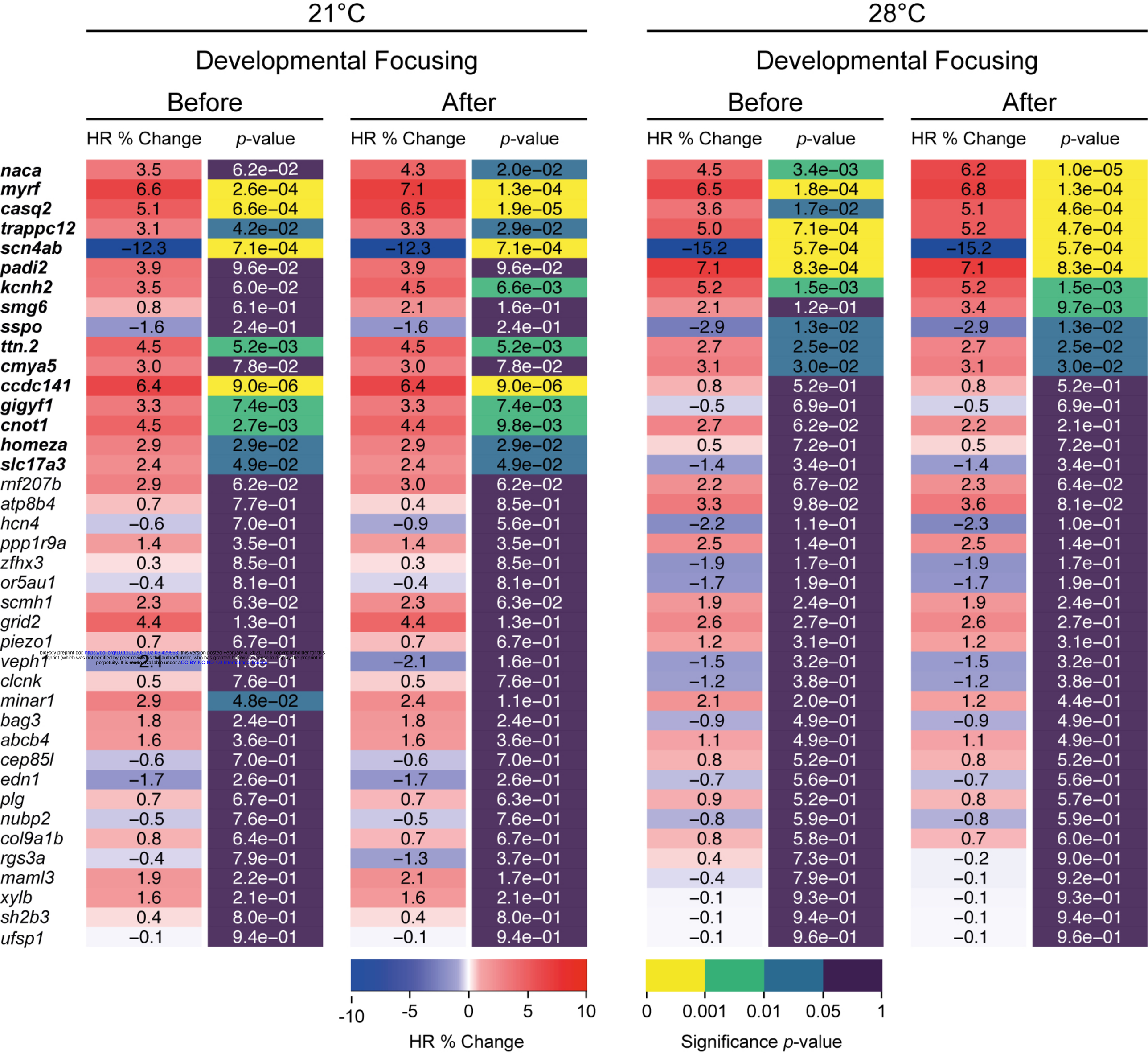

Hammouda et al. Figure S4

Table S1. List of sgRNAs used

Protospacer adjacent motif (PAM) in target sequence enclosed in square brackets "[]"

sgRNA	Target sequence [PAM]
abcb4_T7	ATGTCCCTGAGTGTGAAGAG[TGG]
atp8b4_T2	TAAGTTCTACGATAACACCC[TGG]
bag3_T1	GAGCAGGGCGCCGTTCACCC[GGG]
cabp4_T9	GAATTTGACTACGATGCAGA[TGG]
casq2_T1	TGTTGTCTGGGATGGGTTCG[TGG]
ccdc141_T1	CCAGGAACCTGAAGGTTGTC[AGG]
cdc42_T2	AGAGCGGAGAGAAACTGGCT[CGG]
cep85l _T5	AACCCAGGACTTCTCAGATA[GGG]
clcnk_T10	TTCTCCACTGGAGTAGTTTT[TGG]
cmya5_T1	GTAGAACAGGTAATTCTCGT[TGG]
cnot1_T5	GCCAAGTGTTGACAATACTG[AGG]
col9a1b_T2	GACGGACGCGTAGGCATTCC[AGG]
duox_T3	CATTCGGCACGCTTTCTCTA[AGG]
edn1_T4	GCCGACGGAGTCTGCGCGGA[GGG]
eml6_T2	CTGCGCTGTTCGCACGCTAA[AGG]
gigyf1_T3	GAATGAACCGGCATGAACGC[CGG]
git2_T3	TAAACGCCTTCGAAACACGG[AGG]
grid2_T8	AAAGGCTACGGCTAAGGGTC[TGG]
hcn4_T5	AAACTCCCTTCGAACTTGTG[AGG]
homeza_T1	GCTACCAGCAGGTGCGAGAT[TGG]
kcnh2_T1	CATCACTGCTGGGAGAACCG[GGG]
maml3_T19	TCATGTAAGGTGTCATCATA[GGG]
minar1_T1	GTTGCCGTCGGCGACGCGTA[GGG]
mus81_T7	AAGAGGATGGACGACCTCTG[TGG]
myrf_T1	CCTTATTGGAGTCCATATTG[TGG]
naca_T1	TTGGTCTTAGGCAAGTAACG[GGG]
nkx2-5_T4	GCCGCGGGTCCTCTTCTCCC[AGG]
nkx2-5_T5	CGGACAGACCCAAGCCCCGG[AGG]
nubp2_T4	GAACTGAATGTGGCACTGTT[AGG]
oca2_T3	TTGCAGGAATCATTCTGTGT[GGG]
ogdh_T4	CAAAGCTGGACTTGGCCTCA[GGG]
or124-2_T1	GCCCACGTGGTCTCGTACGC[CGG]
or5au1_T2	GTCATGGACTCTTGCCTGTA[TGG]
padi2_T4	AGACTGGTATTACGGTTAAG[AGG]
piezo1_T1	TTGGGAGCCCGGATGTAGTT[AGG]
plekha8_T9	GCGGTGAAGCTTTCATAACA[CGG]
plg_T1	GGCAACGGGGCCAATTATCG[AGG]
ppp1r9a_T7	TGGTTCTTAGGAGATTCGGG[TGG]
rgs3a_T6	GATCAAGTCACAGTCCAAGA[TGG]

rnf207b_T2	TAGACTTGTTTGTACTGATC[TGG]
scmh1_T2	TCTGACCTGCGCTGTACGAG[TGG]
scn4ab_T2	TTAGGCTTAGCAATCCGCAA[CGG]
sh2b3_T1	AAGAAGTCCGTCGCTGCAAT[CGG]
slc17a3_T5	GTCTTGGCGCCGATTGTGAC[AGG]
smg6_T2	AAAGATAAAACCAAGGGCGT[AGG]
sspo_T4	GTGCACCAAGTCATGTGGTT[GGG]
trappc12_T2	CAACACGCAGTGCCTCAAGC[TGG]
ttl_T1	GCTGGTAAATTACTACAGAG[GGG]
ttn.2_T1	GAGCTAGCTGTCAAAGCCAT[GGG]
ufsp1_T1	GCTGGAGAGCATCGCAGTCC[AGG]
veph1_T1	GGCTCTGGTGGAGGTGTCCC[AGG]
xylb_T1	TTTCCAGTGTCAGTACCTAC[AGG]
zfhx3_T1	AGCTGAGCGCACCCTGCCTG[AGG]

Table S2. List of primers used for genotyping by PCR

sgRNA	**Primers (5' – 3' direction)**
abcb4 Lf	CCTCTGCAGAAGCTGGATGG
abcb4 Lr	TTTGCGATGGCGTGTGAGCG
atp8b4 Lf	ACCTACAGTCAAAGGGAAATGAGC
atp8b4 Lr	ACGCTGCCTCGTCTGGTGAC
bag3 Lf	CTTCGCTTAGGAGCCAGTCC
bag3 Lr	CAGTATGGTCTGAACCCGCC
cabp4 Lf	GTGCCATCTTGCCATGCTGC
cabp4 Lr	ATCCTGCTGCTCCTGGTCCC
casq2 Lf	CGAACAGGTCAAACCGTGTG
casq2 Lr	GGAACTTGCACAAACGGACC
ccdc141 Lf	GGCTACGGATGAAGGAGCTC
ccdc141 Lr	TCCTGGCTAAGTGAAGCAGC
cdc42 Lf	TCCAGAGCTGCGAGGATGGC
cdc42 Lr	CCAGCCGCTCTGTTCTGGGC
cep85l Lf	AGGAGTGAGCTGAGGATGGG
cep85l Lr	GCATCCTCACTCTAGCCGGG
clcnk Lf	GATTCATGCTGTGTTCCCGC
clcnk Lr	CCACTGAGTTGGTCGCTTTG
cmya5 Lf	TTTGTGGGAGCTCGTCTGGG
cmya5 Lr	GCCACGCTGAGATGGAGCCC
cnot1 Lf	CCGGTTGTGGCGCCTTGAGG
cnot1 Lr	GCTTTGGGTCTGGCACTGCG
col9a1b Lf	AGGGACTCACTTACCGGAAGCCC
col9a1b Lr	CTGGTCCTCAGGGAGTGGCAGG
duox Lf	GACGCTGTCAGCTCGCACTG
duox Lr	GGTCCACTCATCGCTCCCTC
edn1 Lf	TCTCCGTGCTGTCAGTGTTC
edn1 Lr	ATGCTGGTTGCCATGGAGTC
eml6 Lf	ACGCCACGGACAGCATGGTC
eml6 Lr	TCACTGACAGCTTTGAAGGTTGACG
gigyf1 Lf	ACAGGAGATAGCAGCAGCAG
gigyf1 Lr	CGTCCCTGATTGTAGATTTGCG
git2 Lf	TTGCTGTCGCCGCTGCTCTG
git2 Lr	GGGCTCATGGGACCTTATGTTGG
grid2 Lf	ACCTACAGACCTGTAACTCCTTCGC
grid2 Lr	ACCTGGAGCACCTACACCACAGG
hcn4 Lf	GACCCGTCAAGTGCCACAGG
hcn4 Lr	CACACCCTCCTTGTCCCTTG
homeza Lf	GCCAAGGAAGACCAAAGAGC

homeza Lr	TCACAAACCTCGCTCTAGGC
kcnh2 Lf	TCGCCCAGGCAAGTCCAACG
kcnh2 Lr	ACCTCATCGCCACTTGAGTGTG
maml3 Lf	CGGCAGCCATGTTGTCGTAC
maml3 Lr	AAGCGGGTTATGTGTGCTGC
minar1 Lf	CGGTCAGCATGAACTAAGCTTCGG
minar1 Lr	TGGAGACGGACAGTGATTCCAGTGG
mus81 Lf	GAAGACGACGAGACGGCCGG
mus81 Lr	TGACCCGAACAGTACCTTTGTG
myrf Lf	GGTCCACCAACCGCCTGCC
myrf Lr	AGCATCCTAGCATTGCAGCC
naca Lf	TCGCTCTCCTCCTGTACTGTAGGG
naca Lr	TCTGAGTCTACTGAAGCCAGCC
nkx2-5 lf	TAGCTTTGAGGCCTGCAGAC
nkx2-5 lr	CGCATAGTTCGTGTTGCAGG
nubp2 Lf	ACTGATGAGCCAGCCAACCC
nubp2 Lr	TGGTCTGTGGCCACATGGTG
oca2 Lf	GTTAAAACAGTTTCTTAAAAAGAACAGGA
oca2 Lr	AGCAGAAGAAATGACTCAACATTTTG
ogdh Lf	GAACACTCGTCTGGCCGGCC
ogdh Lr	TACAGCAAGTCCCGCCCACG
or124-2 Lf	TGAGGCTCAGACCCTCCTGG
or124-2 Lr	ATGCGGTCCGGATGAGCTGG
or5au1 Lf	GCATTCAGCAGTTCTTCTGTCTTC
or5au1 Lr	GGCTTTGATAGATCTGTGTGGAAGC
padi2 Lf	GCATGACACTACCTGAGAATGAAAC
padi2 Lr	AGCCTCAGTCATCTCAGTAAAGC
piezo1 Lf	GCAGCAGCAGGAAGGTCAGG
piezo1 Lr	CCGCTGCATTAGACCACTGC
plekha8 Lf	CTGGCACCTTCCTGTCCAGC
plekha8 Lr	ACGGAAGTCGCCCAAGTCCG
plg Lf	CACAAACACAGCCGCACGCC
plg Lr	GTGGGCGTGTCCGAGTCGAC
ppp1r9a Lf	CGAGGTCCAACCGAGGCAGC
ppp1r9a Lr	TCTCTGTCAGATCTGAGCCGGG
rgs3a Lf	TGAGCTGTGTTCGCCCACTC
rgs3a Lr	GGAGGGCTTCAACTGTGAGG
rnf207b Lf	GCAGAAGCCTCCCATTGACG
rnf207b Lr	CCTCTGGCTGACCGCTCCTG
scmh1 Lf	ACTCTGTTCGAGCGCCTCCC
scmh1 Lr	AGGCGCATCCTGCAGCTTCC
scn4ab Lf	TCACCACTTCTGCAGGATGG
scn4ab Lr	GAGGCGTAGTGATCTGACGG

sh2b3 Lf	TTTCTGCCGGCATCTGCTCC
sh2b3 Lr	CCTGCTGGTCGTTGTCCGTC
slc17a3 Lf	CCGCTGTGCCCAGGAGCAAG
slc17a3 Lr	AGGAAACGACCCGTGACCAC
smg6 Lf	CCCAGCATCAGTGGAGGTGC
smg6 Lr	CCCTGAGCCTCAGTCCCAGC
sspo Lf	TGCAGTCGAGGGTCAGTGGTCG
sspo Lr	CACAGGATCGCGGGCAAGAAGG
trappc12 Lf	GTGCCTGCTGTACCTGGGCC
trappc12 Lr	ACCACCACCCTCTCTCCCAGC
ttl Lf	CCGGGCGGGACCAACAACTG
ttl Lr	GGAGTCAGACAGCTCTGGGC
ttn.2 Lf	CAGAGCTGGACGGACATCGG
ttn.2 Lr	GGAGCGCTGACGTCTGCCTC
ufsp1 Lf	TGGGAAAGGACTAGAGGAGGG
ufsp1 Lr	GACACTCGCTTCCAGGACAC
veph1 Lf	TCTGTCAGAGCGGATGCAAG
veph1 Lr	AGTCTCTGATCGGGATGCAAC
xylb Lf	CCTGCAGCAACATGGCAGTGTG
xylb Lr	ACCATCACTGTGGTCAATGGCTGC
zfhx3 Lf	GGCTGGGTGGTGGGTGTCAG
zfhx3 Lr	TGTGCGGCTAGGTGGTGGAC

Table 1. List of randomly selected genes.

Medaka Ensembl gene names and codes, as well as orthologous human genes as annotated in the 95th Ensembl release.

Ensembl ID	Medaka Gene	Orthologous Human Gene
ENSORLG00000006335	novel gene - *cdc42* (cell division control protein 42 homolog)	na (*CDC42* by name)
ENSORLG00000000979	novel gene - *ogdh* (2-oxoglutarate dehydrogenase)	*OGDH*
ENSORLG00000005268	*duox* (dual oxidase 1)	*DUOX1*
ENSORLG00000007310	*git2* (GIT ArfGAP2)	*GIT2*
ENSORLG00000003492	*mus81* (MUS81 Structure-Specific Endonuclease Subunit)	*MUS81*
ENSORLG00000020766	*or124-2* (odorant receptor, family E 124, member 2)	na
ENSORLG00000007400	*plekha8* (pleckstrin homology domain containing A8)	*PLEKHA8*
ENSORLG00000022757	*ttl* (tubulin tyrosine ligase)	*TTL*
ENSORLG00000005922	*cabp4* (calcium binding protein 4)	*CABP2*
ENSORLG00000023106	novel gene - *eml6* (echinoderm microtubule-associated protein-like 6)	*EML6*

Table 2. List of candidate genes extracted from Human GWAS using GRASP 2.0 Database

Human genes are categorized according to their association into "heart rate" (**bold**) and "non-heart rate" (non bold) related phenotypes in human GWAS.

Human Gene	Coding SNP ID	Associated heart phenotype	Association Reference	Medaka orthologue gene (Ensembl release)	Ensembl Gene Code
ATP8B4	**rs2452524**	**Pulse rate**	**(Hiura et al. 2010)**	***atp8b4*** **(98)**	**ENSORLG00000005106**
CASQ2	**rs4074536**	**QRS interval**	**(Sotoodehnia et al. 2010)**	***casq2*** **(89)**	**ENSORLG00000017885**
CCDC141	**rs17362588**	**Heart rate**	**(Hoed et al. 2013)**	**na (89) (TBLASTN=*ccdc141*)**	**TBLASTN = ENSORLG00000030409**
CEP85L	**rs3734381**	**QRS interval**	**(Sotoodehnia et al. 2010)**	***cep85l*** **(91)**	**ENSORLG00000015455**
CMYA5	**rs10942901**	**Heart rate**	**(Hoed et al. 2013)**	***cmya5*** **(91)**	**ENSORLG00000008983**
COL9A1	**rs592121**	**Pulse rate**	**(Hiura et al. 2010)**	***col9a1b*** **(98)**	**ENSORLG00000010431**
GIGYF1	**rs221794**	**Heart rate**	**(Hoed et al. 2013)**	***gigyf1*** **(89)**	**ENSORLG00000003655**
GRID2	**rs1385405**	**Pulse rate**	**(Hiura et al. 2010)**	***grid2*** **(98)**	**ENSORLG00000024663**
HOMEZ	**rs1055061**	**Sick sinus syndrome**	**(Holm et al. 2011)**	***homeza*** **(89)**	**ENSORLG00000012220**
KCNH2	**rs1805123**	**QT interval**	**(Pfeufer et al. 2009)**	***kcnh2*** **(98)**	**ENSORLG00000004137**
MINAR1	**rs2297773**	**Pulse rate**	**(Hiura et al. 2010)**	***minar1*** **(98)**	**ENSORLG00000016707**
MYRF	**rs174535**	**RR interval**	**(Eijgelsheim et al. 2010)**	***myrf*** **(91)**	**ENSORLG00000006459**
NACA	**rs2926743**	**Heart rate**	**(Hoed et al. 2013)**	***naca*** **(98)**	**ENSORLG00000012246**
OR5AU1	**rs4982419**	**Pulse rate**	**(Hiura et al. 2010)**	**na (98) (TBLASTN=no name)**	**TBLASTN = ENSORLG00000024679**
PADI4	**rs2240335**	**Pulse rate**	**(Hiura et al. 2010)**	**na (98) (TBLASTN=*padi2*)**	**TBLASTN = ENSORLG00000007539**
PPP1R9A	**rs854524**	**Pulse rate**	**(Hiura et al. 2010)**	***ppp1r9a*** **(98)**	**ENSORLG00000004418**
RNF207	**rs846111**	**QT interval**	**(Newton-Cheh et al. 2009)**	***rnf207b*** **(91)**	**ENSORLG00000017207**
SCN5A	**rs1805126**	**QRS interval**	**(Ritchie et al. 2013)**	**na (89) (TBLASTN=*scn4ab*)**	**TBLASTN = ENSORLG00000003273**
SSPO	**rs10261977**	**Pulse rate**	**(Hiura et al. 2010)**	***sspo*** **(98)**	**ENSORLG00000004121**
TRAPPC12	**rs6767**	**Pulse rate**	**(Hiura et al. 2010)**	***trappc12*** **(98)**	**ENSORLG00000017859**
TTN	**rs12476289**	**QT interval**	**(Marroni et al. 2009)**	***ttn.2*** **(91)**	**ENSORLG00000018144**
UFSP1	**rs12666989**	**RR interval**	**(Eijgelsheim et al. 2010)**	**na (89) (TBLASTN=*ufsp1*)**	**TBLASTN = ENSORLG00000022928**
XYLB	**rs17118**	**PR interval**	**(Smith et al. 2009)**	***xylb*** **(91)**	**ENSORLG00000003755**
ABCB1	rs1128503	Drug response CVD	(Paré et al. 2013)	*abcb4* (91)	ENSORLG00000009269
BAG3	rs3858340	Sporadic dilated cardiomyopathy	(Villard et al. 2011)	*bag3* (89)	ENSORLG00000013813
CLCNKA	rs1805152	Sporadic dilated cardiomyopathy	(Villard et al. 2011)	*clcnk* (89)	ENSORLG00000018693
CNOT1	rs11866002	Aortic valve calcium	(Thanassoulis et al. 2013)	*cnot1* (91)	ENSORLG00000013734

EDN1	rs150035515	Aortic valve calcium	(Matsa et al. 2014)	*edn1* (89)	ENSORLG00000009276
HCN4	rs529004	Aortic valve calcium	(Thanassoulis et al. 2013)	*hcn4* (91)	ENSORLG00000013180
MAML3	rs11729794	Congenital heart malformations	(Hu et al. 2013)	na (91) (TBLASTN=*maml3*)	TBLASTN = NCBI Ref Seq: XM_023954746.1
NUBP2	rs344359	LV systolic dysfunction	(Vasan et al. 2009)	*nubp2* (91)	ENSORLG00000007228
PIEZO1	rs2290902	Bicuspid aortic valve	(Wooten et al. 2010)	*piezo1* (91)	ENSORLG00000000402
PLG	rs13231	Aortic valve calcium	(Thanassoulis et al. 2013)	*plg* (91)	ENSORLG00000020532
RGS3	rs12341266	Hypertrophic cardiomyopathy	(Wooten et al. 2013)	*rgs3a* (91)	ENSORLG00000006823
SCMH1	rs10489520	Ischemic stroke	(Ikram et al. 2009)	*scmh1* (91)	ENSORLG00000014207
SH2B3	rs3184504	Tetrology of fallot	(Cordell et al. 2013)	*sh2b3* (91)	ENSORLG00000003569
SLC17A3	rs942379	Bicuspid aortic valve	(Wooten et al. 2010)	*si:ch1073-513e17.1* (91)	ENSORLG00000007671
SMG6	rs216193	Aortic root size	(Vasan et al. 2009)	*smg6* (91)	ENSORLG00000003317
VEPH1	rs1378796	Sporadic dilated cardiomyopathy	(Villard et al. 2011)	*veph1* (89)	ENSORLG00000012452
ZFHX3	rs2228200	Aortic valve calcium	(Thanassoulis et al. 2013)	*zfhx3* (91)	ENSORLG00000007874